



Ana Tellechea,^{1,2} Ermelindo C. Leal,^{1,2} Antonios Kafanas,¹ Michael E. Auster,¹ Sarada Kuchibhotla,¹ Yana Ostrovsky,¹ Francesco Tecilazich,¹ Dimitrios Baltzis,¹ Yongjun Zheng,¹ Eugénia Carvalho,^{1,2} Janice M. Zabolotny,¹ Zuyi Weng,³ Anastasia Petra,³ Arti Patel,³ Smaro Panagiotidou,³ Leena Pradhan-Nabzdyk,¹ Theoharis C. Theoharides,³ and Aristidis Veves¹

Mast Cells Regulate Wound Healing in Diabetes



Diabetes 2016;65:2006–2019 | DOI: 10.2337/db15-0340

Diabetic foot ulceration is a severe complication of diabetes that lacks effective treatment. Mast cells (MCs) contribute to wound healing, but their role in diabetes skin complications is poorly understood. Here we show that the number of degranulated MCs is increased in unwounded forearm and foot skin of patients with diabetes and in unwounded dorsal skin of diabetic mice ($P < 0.05$). Conversely, postwounding MC degranulation increases in nondiabetic mice, but not in diabetic mice. Pretreatment with the MC degranulation inhibitor disodium cromoglycate rescues diabetes-associated wound-healing impairment in mice and shifts macrophages to the regenerative M2 phenotype ($P < 0.05$). Nevertheless, nondiabetic and diabetic mice deficient in MCs have delayed wound healing compared with their wild-type (WT) controls, implying that some MC mediator is needed for proper healing. MCs are a major source of vascular endothelial growth factor (VEGF) in mouse skin, but the level of VEGF is reduced in diabetic mouse skin, and its release from human MCs is reduced in hyperglycemic conditions. Topical treatment with the MC trigger substance P does not affect wound healing in MC-deficient mice, but improves it in WT mice. In conclusion, the presence of non-degranulated MCs in unwounded skin is required for proper wound healing, and therapies inhibiting MC degranulation could improve wound healing in diabetes.

Foot ulceration and associated impaired wound healing is a major problem in patients with diabetes that significantly impairs their life quality, leading to prolonged hospitalization and often resulting in lower extremity amputations

(1,2). Wound healing is a complex, dynamic process that involves coordinated and overlapping phases, including coagulation-inflammation, proliferation, and maturation (3). Chronic wounds in patients with diabetes become stalled mainly in the inflammatory phase and do not progress to the next phases of wound healing (3–5). We previously showed that increased skin inflammation and aberrant growth factor levels contribute to healing failure in individuals with diabetes (6).

Mast cells (MCs) are bone marrow progenitor-derived immune cells that mature in tissues. MCs are greatly affected by the local microenvironment (7,8) and can participate in numerous biological processes, including inflammation and neovascularization, through the release of several mediators (9,10). MCs interact with macrophages, endothelial cells, and fibroblasts, and there is evidence supporting their participation in wound healing (11–14). During the inflammatory phase, MCs recruit neutrophils to the site of injury (12–15) and secrete cytokines that activate tissue-resident macrophages (16). During the proliferative phase, MCs stimulate fibroblast proliferation via interleukin (IL)-4, vascular endothelial growth factor (VEGF), and basic fibroblast growth factor (17) and promote wound tissue granulation, cell migration, angiogenesis, and collagen maturation (18–20).

There is little information on the number and activation state of skin MCs in diabetes. MCs are localized around blood vessels and in fat depots, where they influence local inflammation and adipocytokine release (21,22) and can cause insulin-induced local lipodystrophy (23). MCs are also close to peripheral sensory nerves (24) and can be

¹Beth Israel Deaconess Medical Center, Harvard Medical School, Boston, MA

²Center for Neuroscience and Cell Biology, University of Coimbra, Coimbra, Portugal

³Molecular Immunopharmacology and Drug Discovery Laboratory, Department of Integrative Physiology and Pathobiology, Tufts University School of Medicine, Boston, MA

Corresponding author: Aristidis Veves, aveves@bidmc.harvard.edu.

Received 11 March 2016 and accepted 2 April 2016.

This article contains Supplementary Data online at <http://diabetes.diabetesjournals.org/lookup/suppl/doi:10.2337/db15-0340/-/DC1>.

© 2016 by the American Diabetes Association. Readers may use this article as long as the work is properly cited, the use is educational and not for profit, and the work is not altered.

stimulated by substance P (SP), which, together with IL-33, causes VEGF release (25). Furthermore, MCs affect macrophages and contribute to diet-induced obesity and diabetes (22). Macrophage phenotype can be broadly characterized as “proinflammatory” M1 or “immunomodulatory/regenerative” M2 (26,27). M1 activation is required during the acute inflammatory phase but is also present in chronic wounds characterized by persistent inflammation (28), whereas M2 activation during the proliferative phase promotes angiogenesis and collagen production (29).

We recently reported that chronic inflammation in the skin of humans with diabetes or in experimental diabetes models (6,30) and defective inflammation resolution in diabetic mouse wounds (31) impair the healing process. Here we hypothesized that chronic MC degranulation in the skin of diabetes subjects contributes to abnormal healing and that correcting this condition could rescue wound-healing impairment. To this end, we first examined skin MC degranulation and macrophage activation phenotype in human and experimental diabetes. We then investigated the mechanisms through which MCs affect wound healing in nondiabetic and diabetic wild-type (WT) and MC-deficient mice, as well as in human MC cultures.

RESEARCH DESIGN AND METHODS

Human Studies

Subjects

Skin and serum specimens were obtained from 10 subjects without diabetes (mean \pm SD age 60 ± 5 years, 3 males, mean BMI 28.6 ± 8.6 kg/m²) and 56 subjects with diabetes (mean age 57 ± 8 years, 41 male, BMI 33.4 ± 6.9 kg/m², 21 with type 1 diabetes, mean duration of diabetes 20 ± 25 years). Peripheral diabetic neuropathy was present in 48 patients with diabetes (86%), while the nerve axon reflex, an index of subclinical peripheral neuropathy, was reduced at the forearm level of patients with diabetes.

Skin Specimens

Forearm Skin Biopsies. Two-millimeter forearm skin biopsy samples were obtained from the population described above. Five-micrometer sections were used to evaluate total and degranulated MCs by toluidine blue staining (0.1%, pH 2) and by immunohistochemistry for MC tryptase using anti-AA1 antibody (Abcam, Cambridge, MA).

Foot Skin Specimens. Nonlesional discarded skin specimens were collected during elective foot surgeries from five subjects without diabetes and six subjects with diabetes. We evaluated MCs as described for the forearm skin biopsies; HLA-DR⁺/CD68⁺ M1 and CD206⁺/CD68⁺ M2 macrophages by immunofluorescence; and tumor necrosis factor- α (TNF- α), IL-1 β , and IL-10 mRNA by quantitative real-time RT-PCR (qRT-PCR).

Serum Samples

From the same population, IL-6 and TNF- α serum levels were measured using a Luminex 200 apparatus (Luminex, Austin, TX) and multiplex immunoassay panels (Millipore, Chicago, IL).

Written informed consent was received from all subjects. The protocol was approved by the Institutional Review Board of Beth Israel Deaconess Medical Center (BIDMC).

Animal Studies

Mouse Models

Male C57BL/6J and MC-deficient WBB6F1/J-Kit^W/Kit^{W-v} mice, together with their WBB6F1/J-Kit^{+/+} controls, were purchased from The Jackson Laboratory (Bar Harbor, ME). To induce diabetes, 8-week-old mice ($N = 10$ –12/group) received 50 mg/kg streptozotocin (STZ) intraperitoneally daily for 5 days in citrate buffer (0.1 mol/L). Mice in the nondiabetic groups ($N = 10$ –12/group) received vehicle at the same age. Fasting blood glucose levels were monitored 10 days post-STZ, and mice with levels >250 mg/dL were considered to have diabetes. All mice were considered to have diabetes 10 days post-STZ. To evaluate the effect of MC degranulation inhibition, C57BL/6J nondiabetic and diabetic mice were treated for 10 days prior to wounding with the MC stabilizer disodium cromoglycate (DSCG) 50 mg/kg i.p. daily as previously described (22). To use a different mouse model of MC deficiency, Kit^{W-sh}/Kit^{W-sh} mice were generated from breeder mice obtained from The Jackson Laboratory. B6.Cg-Kit^{W-sh}/HNhrJaeBsmJ females were crossed with C57BL/6J males. The heterozygotes from the first generation were then intercrossed, and the resulting homozygotes were selected. Age-matched male Kit^{W-sh}/Kit^{W-sh} mice and their respective B6.Cg controls from the colony were used ($N = 12$ /group).

Wound Creation, Monitoring, and Treatment

All mice were the same age (16 weeks old) at the time of wounding. In the diabetes groups, all mice had the same duration of diabetes (8 weeks). Eight weeks after STZ or vehicle treatment, at 16 weeks of age, mice were anesthetized using ketamine (100 mg/kg i.p.) and xylazine (10 mg/kg i.p.) and two circular 6-mm full-thickness wounds were created on their shaved dorsum. Wound closure was monitored daily for 10 days by measuring the wound size using acetate tracing followed by ImageJ software (National Institutes of Health, Bethesda, MD) analysis. Data are presented as a percentage of original wound size. Day 10 wound size results were confirmed by digital imaging. For the SP studies, one of the wounds in each mouse received daily topical SP in saline solution (32 μ g/5 μ L), while the other received saline solution. Mice were euthanized at day 10.

Tissue Collection

At day 0, the skin biopsy samples were collected. At day 10, 1 \times 1 cm skin sections, including the wound margins, were harvested. Specimens were further divided into four sections. For histology and immunohistochemistry, tissue was fixed in 10% formalin and subsequently formalin fixed and paraffin embedded. For immunofluorescence, skin was embedded in an optimal cutting temperature compound and gradually frozen on dry ice, then stored at -80°C .

For protein and mRNA analysis, tissue was snap frozen in liquid nitrogen and stored at -80°C .

Skin Histological Analysis and Immunohistochemistry

For morphologic analysis, 5- μm formalin fixed and paraffin embedded sections were stained with hematoxylin-eosin. For wound tissues, only sections including both wound margin and the periwound area were analyzed to ensure consistency. Wound reepithelialization was assessed by an experienced pathologist (A.K.) and was scored as follows: 0, no reepithelialization (no migrating epithelial tongue from the wound margin); 1, incomplete reepithelialization (migrating epithelial tongue not fully covering the wound bed); and 2, full re-epithelialization (wound bed fully covered by new epidermis). For MC evaluation, sections were deparaffinized and stained with 0.1% toluidine blue, pH 2. CD31 staining was performed as previously described by us (30). Five-micrometer frozen skin sections were costained with CD68 (Abcam), TNF- α (Serotec, Oxford, U.K.), and inducible nitric oxide synthase (Abcam) for M1 macrophages, or with CD68 and CD206 (Santa Cruz Biotechnology, Santa Cruz, CA) and arginase-1 (Santa Cruz Biotechnology) for M2 macrophages. Each sample was counterstained with DAPI. To assess specificity, staining was first performed separately for M0, M1, and M2 macrophages, with and without primary and secondary antibodies. Next, staining for M0 with secondary antibodies to M1 and M2 was performed to assess cross-reactivity. Finally, all primary antibodies (against the M0, M1, and M2 markers) were used, but only the secondary antibody for the M0 antibody was added. A water control was used to assess autofluorescence. All analysis was performed in a blinded fashion.

Skin Protein Analysis

Sample preparation, protein quantification, and Western blot analysis were performed as previously described by us (31). Target proteins were detected with anti-VEGF (Abcam) and anti-matrix metalloproteinase-9 (MMP-9) antibodies (Abcam), followed by horseradish peroxidase-conjugated secondary antibodies (Sigma-Aldrich, St. Louis, MO; and Abcam). For quantification, band densitometry was normalized to β -actin (Sigma-Aldrich) using ImageJ software.

Gene Expression

Standard qRT-PCR was performed as previously described by us (31). Primer sequences (Supplementary Table 1) were obtained from Integrated DNA Technologies (Coralville, IA). Target gene levels were normalized to 18 S levels.

All animal studies were approved by the Institutional Animal Care and Use Committee of BIDMC.

Cell Culture Studies

Human MC Culture

LAD2 cells were cultured in StemPro-34 SFM Medium $1\times$ (5.5 mmol/L glucose) (Invitrogen, Carlsbad, CA) supplemented with 100 ng/mL recombinant human stem cell factor (Swedish Orphan Biovitrum AB, Stockholm, Sweden) and 1 unit/mL penicillin/streptomycin, at 37°C with 5% CO_2 .

StemPro-34 SFM Medium was supplemented with 24.5 mmol/L glucose solution for a final concentration of 30 mmol/L to prepare high-glucose (HG) media or 24.5 mmol/L mannitol (osmotic control) to prepare normal-glucose (NG) media. Media were prepared as fresh solutions and supplemented with the sugars immediately before use. Cells were maintained in HG or NG conditions for 2 weeks before the studies.

MC Degranulation

β -Hexosaminidase (β -hex) release was evaluated using a fluorometric assay. LAD2 cells (0.5×10^5 /tube) were stimulated for 30 min with SP (1 $\mu\text{mol/L}$), supernatant fluids were collected, and cell pellets were lysed with 1% Triton X-100. Supernatants and cell lysates were incubated in reaction buffer (*p*-nitrophenyl-*N*-acetyl- β -D-glucosaminide; Sigma-Aldrich) for 1.5 h; 0.2 mol/L glycine was added to stop the reaction. Absorbance was measured at 405 nm, and results were expressed as the percentage of β -hex released over the total.

MC Mediator Release

LAD2 cells were triggered with SP (1 $\mu\text{mol/L}$) for 24 h. VEGF, IL-8, TNF- α , and MCP-1 were measured in the supernatant fluids using ELISA assay kits (R&D Systems).

Statistical Analysis

The statistical power analysis was based on preliminary data or data from other studies in our unit. For parametrically distributed data, differences among experimental groups were analyzed using a Student *t* test (for single comparisons) or one-way ANOVA followed by Fisher post hoc test (for multiple comparisons). For nonparametrical data, Mann-Whitney and Kruskal-Wallis tests were used. The Pearson correlation coefficient was calculated. Statistical analysis was performed using Minitab (State College, PA) software, and significance was defined at $P < 0.05$. Results are expressed as the mean \pm SEM.

RESULTS

Human Studies

Skin MC Degranulation Is Increased in Patients With Diabetes and Correlates With Inflammation

To study the number and activation state of MCs in the skin of patients with diabetes, we analyzed forearm and foot skin specimens from patients with diabetes and subjects without diabetes. Forearm skin from patients with diabetes showed increased numbers of total and degranulated MCs by toluidine blue staining (Fig. 1A–C). Results were confirmed by tryptase immunohistochemistry in a subset of the population described above (Supplementary Fig. 1). MC degranulation, assessed by tryptase immunostaining, was also increased in the foot skin of patients with diabetes (Fig. 1D and E), whereas no differences in total MCs were observed (Fig. 1F). In addition, MC degranulation positively correlated with the dermis inflammatory cell number (Fig. 1G) and circulating levels of the inflammatory markers IL-6 and TNF- α (Fig. 1H and I). There were no differences in MC degranulation between type 1 and type 2 diabetes or males and females.

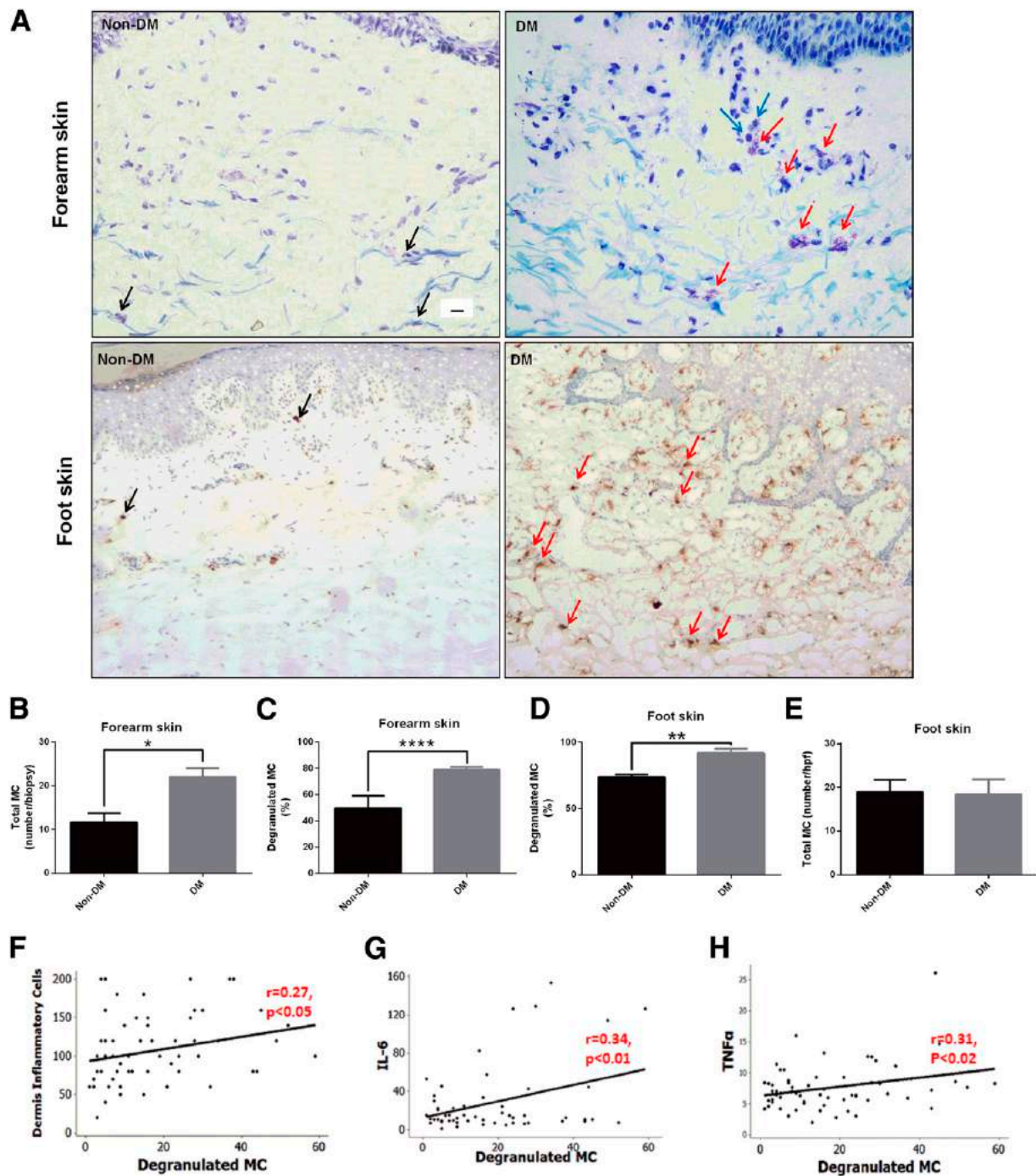


Figure 1—Skin MC degranulation, assessed by toluidine blue and/or tryptase immunostaining, is increased in patients with diabetes and is associated with inflammation. A: Representative images of toluidine blue–stained MCs in forearm skin (top panel) and of tryptase-immunostained MCs in foot skin specimens (bottom panel) from subjects without diabetes (Non-DM) and with diabetes (DM). Scale bar: 10 μ m. Black arrows show nondegranulated MCs, and red arrows show degranulated MCs. Degranulated MCs were in proximity with inflammatory cells (blue arrows). The total number (B) and percentage (C) of degranulated MCs stained with toluidine blue were increased in forearm skin specimens from patients with diabetes. MC degranulation was also increased in foot skin specimens from subjects with diabetes stained with tryptase (D), while the total number of MCs was not different (E). * $P < 0.05$, ** $P < 0.01$, and **** $P < 0.0001$. A positive correlation was observed between degranulated MCs and the dermis inflammatory cells (F), and the serum levels of IL-6 (G) and TNF- α (H). hpf, high power field (400 \times magnification).

Skin Macrophage Phenotype Is Polarized Toward M1 in Patients With Diabetes

To assess the macrophage phenotype in the skin of patients with diabetes, we evaluated M1 and M2 macrophage

numbers in forearm and foot skin specimens from subjects with diabetes and without diabetes (Fig. 2A–C). The number of M1 macrophages was increased in forearm skin from subjects with diabetes when compared with subjects without

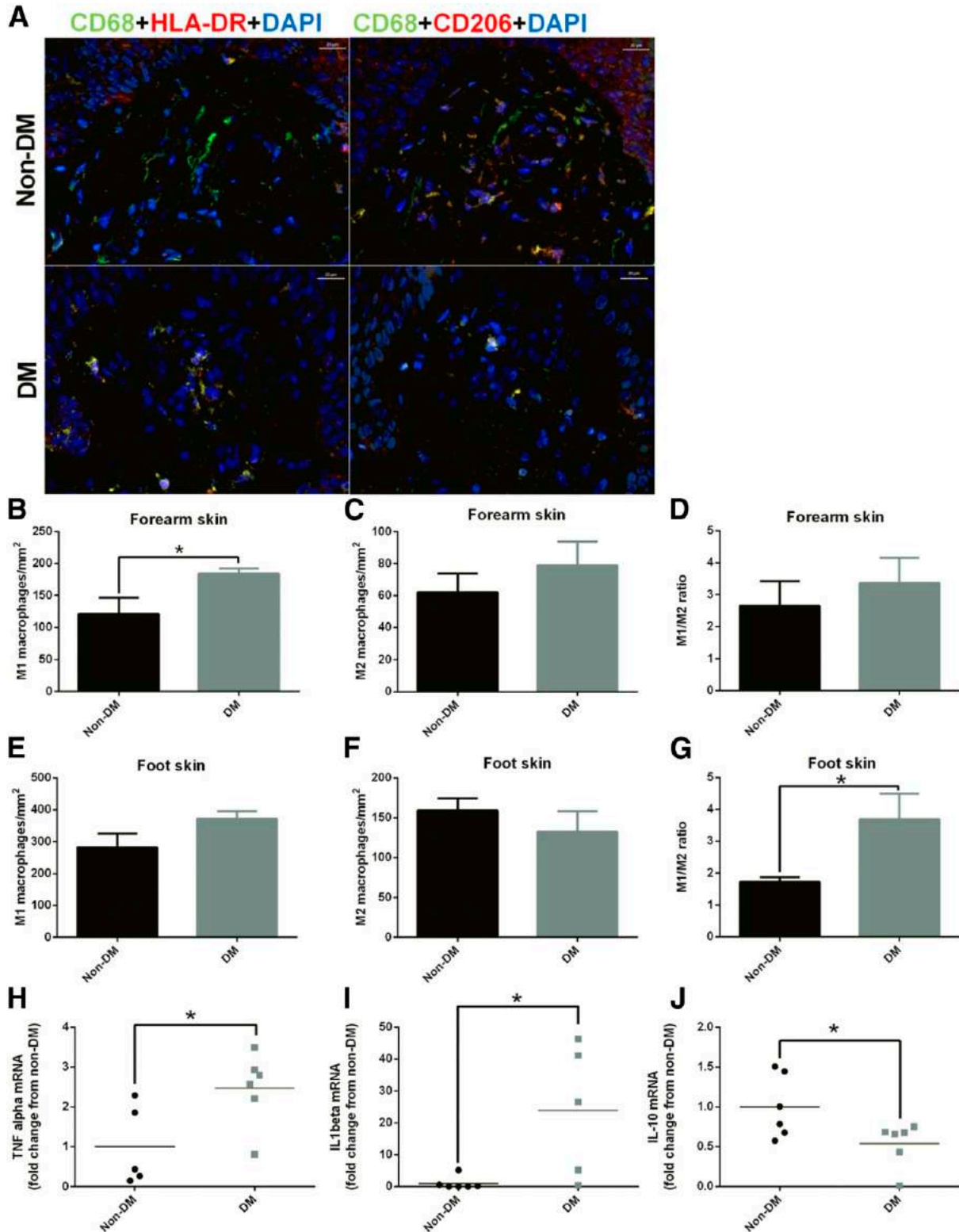


Figure 2—Skin macrophage phenotype is polarized toward M1 in patients with diabetes. **A**: Representative images of M1 and M2 macrophages in foot skin specimens from subjects without diabetes (Non-DM) and with diabetes (DM). Scale bar: 20 μ m. M1 (left panel CD68⁺HLADR⁺DAPI) and M2 (right panel CD68⁺CD206⁺DAPI) are shown in yellow-orange as a result from the triple-positive staining. In the forearm skin, the number of M1 macrophages was increased in subjects with diabetes (**B**), whereas the number of M2 macrophages (**C**) and the M1/M2 ratio (**D**) were not different. In the foot skin, the number of M1 macrophages tended to be increased in subjects with diabetes (**E**), whereas the number of M2 macrophages tended to be reduced (**F**), resulting in a higher M1/M2 ratio (**G**). mRNA expression of the M1 markers TNF- α (**H**) and IL-1 β (**I**) was increased, whereas the expression of M2 marker IL-10 was reduced (**J**) in the foot skin of patients with diabetes. * $P < 0.05$.

diabetes (Fig. 2B), whereas no differences were observed in M2 (Fig. 2C). At the foot level, the dermal M1/M2 ratio was increased in subjects with diabetes (Fig. 2G). Moreover, mRNA expression of the M1-associated proinflammatory cytokines TNF- α (Fig. 2H) and IL-1 β (Fig. 2I) was elevated in the foot skin of subjects with diabetes, whereas the M2-associated anti-inflammatory cytokine IL-10 was reduced (Fig. 2J).

Animal Studies

Skin MC Degranulation Is Increased in Diabetic Mice

To determine the effect of diabetes on dermal MCs, we examined MC degranulation in nondiabetic and diabetic C57BL/6J mouse skin before (day 0) and 10 days postwounding (day 10) (Fig. 3A–C). Day 0 diabetic mouse skin showed extensive MC degranulation compared with that in nondiabetic mice (Fig. 3A and B). Treatment with the MC degranulation inhibitor DSCG intraperitoneally for 10 days prior to wounding reduced MC degranulation in diabetic mice at day 0, restoring it to levels seen in nondiabetic mice (Fig. 3B). At day 10, no differences were observed between groups (Fig. 3C), mainly because of the fact that although MC degranulation markedly increased from day 0 to day 10 in nondiabetic mice, it did not change in diabetic nontreated mice (Fig. 3D). As a result, the difference in MC degranulation between day 10 and day 0 was markedly reduced in the diabetic mice not treated when compared with all other groups (Fig. 3D). To evaluate skin MC degranulation at an earlier postinjury time point, we used nondiabetic and diabetic C57BL/6J mouse skin specimens that were collected before (day 0) and 3 days after wounding (day 3). In this set of mice, MC degranulation was again elevated in the diabetes group at day 0 (Fig. 3E). At day 3, MC degranulation was similar in nondiabetic and diabetic mice (Fig. 3F), resulting in changes between day 3 and day 0 that were comparable to the changes between day 10 and day 0 (Fig. 3G).

DSCG Pretreatment Accelerates Wound Healing in Diabetic Mice

To evaluate the effect of DSCG on wound healing, we monitored wound closure for 10 days in C57BL/6J nondiabetic and diabetic mice that had been pretreated with DSCG or that were not pretreated. Diabetic mice showed delayed wound closure when compared with nondiabetic mice, but DSCG pretreatment accelerated wound closure in diabetic mice from day 6 to day 10 postwounding, achieving a healing profile similar to that of nondiabetic mice (Fig. 4A and B). DSCG had no significant effect in nondiabetic mice, which showed minimal prewounding MC degranulation.

Wound Healing Is Impaired in MC-Deficient Mice

To study the effect of MC deficiency on wound healing, we evaluated wound closure in MC-deficient *Kit^W/Kit^{W-v}* mice, which possess a c-kit mutation, and their WBB6F1/J controls, with or without diabetes. Compared with WBB6F1/J, healing was delayed in *Kit^W/Kit^{W-v}* mice, from day 5 to day 10 postwounding (Fig. 4C and D). Diabetic *Kit^W/Kit^{W-v}* mice also showed delayed wound closure from day 8 to

day 10 (Fig. 4E and F). To exclude the possibility that the observed healing impairment could be specific to this particular model, we used another MC-deficient mouse model, the *Kit^{W-sh}/Kit^{W-sh}* mice. *Kit^{W-sh}/Kit^{W-sh}* mice have an inversion mutation upstream of the c-kit promoter region, and its phenotype, in contrast with *Kit^W/Kit^{W-v}* mice, has normal levels of other differentiated hematopoietic and lymphoid cells (32,33). Compared with their B6.Cg controls, *Kit^{W-sh}/Kit^{W-sh}* mice showed an even more pronounced healing impairment, from day 1 to day 10 postwounding (Fig. 4G and H).

SP Treatment Accelerates Wound Healing in WT Mice but Not in MC-Deficient Mice

Previous studies in our laboratory have shown that topical SP improves wound healing in nondiabetic and diabetic C57BL/6J mice (31). Here we investigated the effect of SP treatment in nondiabetic and diabetic WBB6F1/J mice and in *Kit^W/Kit^{W-v}* mice. SP treatment accelerated healing in nondiabetic and diabetic WBB6F1/J mice (Fig. 4D and F). However, no differences were observed between nontreated and SP-treated wounds in *Kit^W/Kit^{W-v}* mice (Figs. 4D and F).

Wound Re-Epithelialization and Neovascularization Are Increased in DSCG Pretreated Diabetic Mice and Reduced in *Kit^W/Kit^{W-v}* Mice

To further evaluate the effect of DSCG or MC deficiency on wound healing, we evaluated wound re-epithelialization, granulation, and neovascularization. Day 10 wound re-epithelialization was reduced in C57BL/6J diabetic mice when compared with nondiabetic mice (Fig. 5A and B). More importantly, DSCG pretreatment increased re-epithelialization in diabetic mouse wounds (Fig. 5A and B). Similar to the C57BL/6J strain, re-epithelialization was reduced in WBB6F1/J diabetic mice when compared with their respective nondiabetic controls (Fig. 5C). In addition, both nondiabetic and diabetic *Kit^W/Kit^{W-v}* mouse wounds had lower re-epithelialization than their WBB6F1/J controls, whereas diabetic *Kit^W/Kit^{W-v}* mouse wounds had lower re-epithelialization than nondiabetic *Kit^W/Kit^{W-v}* mouse wounds (Fig. 5C). Furthermore, *Kit^{W-sh}/Kit^{W-sh}* wounds had less granulation tissue than their B6.Cg controls, whereas *Kit^W/Kit^{W-v}* wounds tended to show less granulation than WBB6F1/J controls but failed to reach statistical significance (data not shown). DSCG increased wound neovascularization in C57BL/6J diabetic mice (Fig. 5D and E) but had no major effect on wound granulation (data not shown).

M1/M2 Macrophage Ratio Is Increased in Diabetic Mouse Wounds, and DSCG Restores It to Nondiabetic Levels

To study the macrophage phenotype, we evaluated M1 and M2 macrophage numbers in day 10 periwound skin of C57BL/6J nondiabetic and diabetic mice, pretreated or not with DSCG (Fig. 6A–D). Using TNF- α as the M1 marker and CD206 as the M2 marker, diabetic mice tended to have higher numbers of M1 macrophages

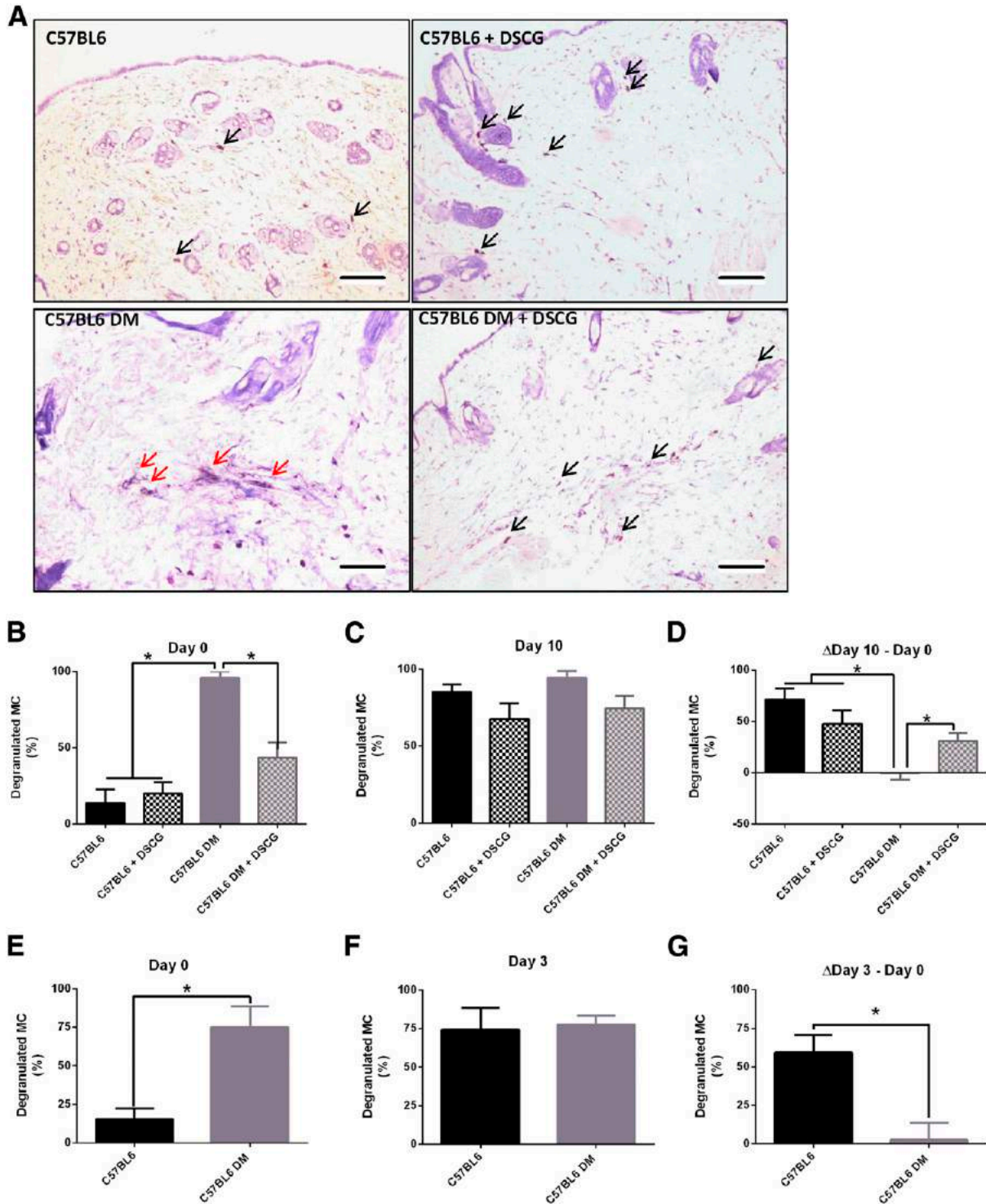


Figure 3—MC degranulation is increased in unwounded skin of diabetic (DM) mice and fails to further increase after wounding. *A*: Representative images of nondegranulated (black arrows) and degranulated (red arrows) MCs in day 0 skin biopsy specimens from C57BL/6J nondiabetic and diabetic mice, untreated and pretreated with DSCG. Scale bar: 100 μ m. *B*: MC degranulation was increased in diabetic mice at day 0 and after intraperitoneal DSCG treatment for 10 days before wounding reduced it. *C*: Nondiabetic mice showed increased MC degranulation at day 10 when compared with day 0, but there were no changes in diabetic mice between days 0 and 10. As a result, there were no differences among the various groups at day 10. *D*: When the difference between days 10 and 0 was calculated, a significant increase was noticed in nondiabetic mice, regardless of whether they were treated with DSCG or not. However, no difference was observed in the diabetic mice not treated with DSCG, but this difference was restored in the DSCG-treated diabetic mice. *E–G*: Similar results were observed in a different set of nondiabetic and diabetic mice that were studied at day 3 postwounding. Thus, MC degranulation was also increased in the skin in diabetic mice on day 0 (*E*), but was not different at day 3 (*F*), resulting in a failure to increase MC degranulation from day 0 to day 3 postwounding in diabetic mice (*G*). * $P < 0.05$.

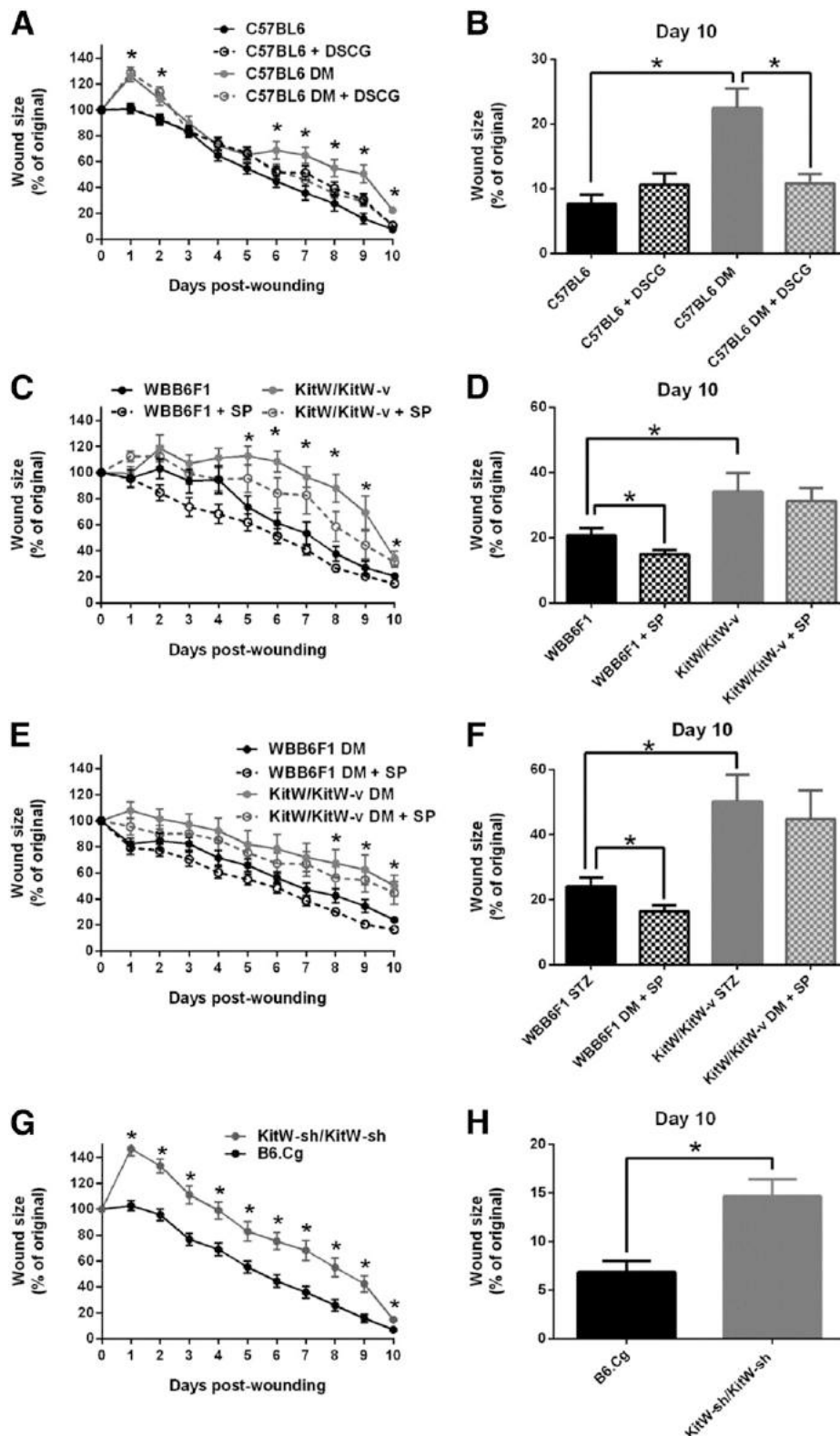


Figure 4—Functional MCs are required for proper wound healing. Wound-healing progress was evaluated over a 10-day period in nondiabetic and diabetic mice treated with DSCG or not treated and MC-deficient mice. *A* and *B*: Wound healing was delayed in C57BL6 diabetic mice compared with nondiabetic mice and DSCG pretreatment accelerated it from days 6 to 10 postwounding. DSCG had no effect on nondiabetic mice. *C*–*F*: Wound healing was delayed in *Kit^W/Kit^{W-v}* mice without or with diabetes, when compared with their respective nondiabetic or diabetic WBB6F1 controls. Topical SP improved healing at day 10 postwounding in both nondiabetic and diabetic WBB6F1 mice, but failed to have an effect in either nondiabetic *Kit^W/Kit^{W-v}* or diabetic *Kit^W/Kit^{W-v}* mice. *G* and *H*: Wound healing was delayed in MC-deficient *Kit^{W-sh}/Kit^{W-sh}* mice when compared with their respective B6.Cg controls. **P* < 0.05. DM, diabetic.

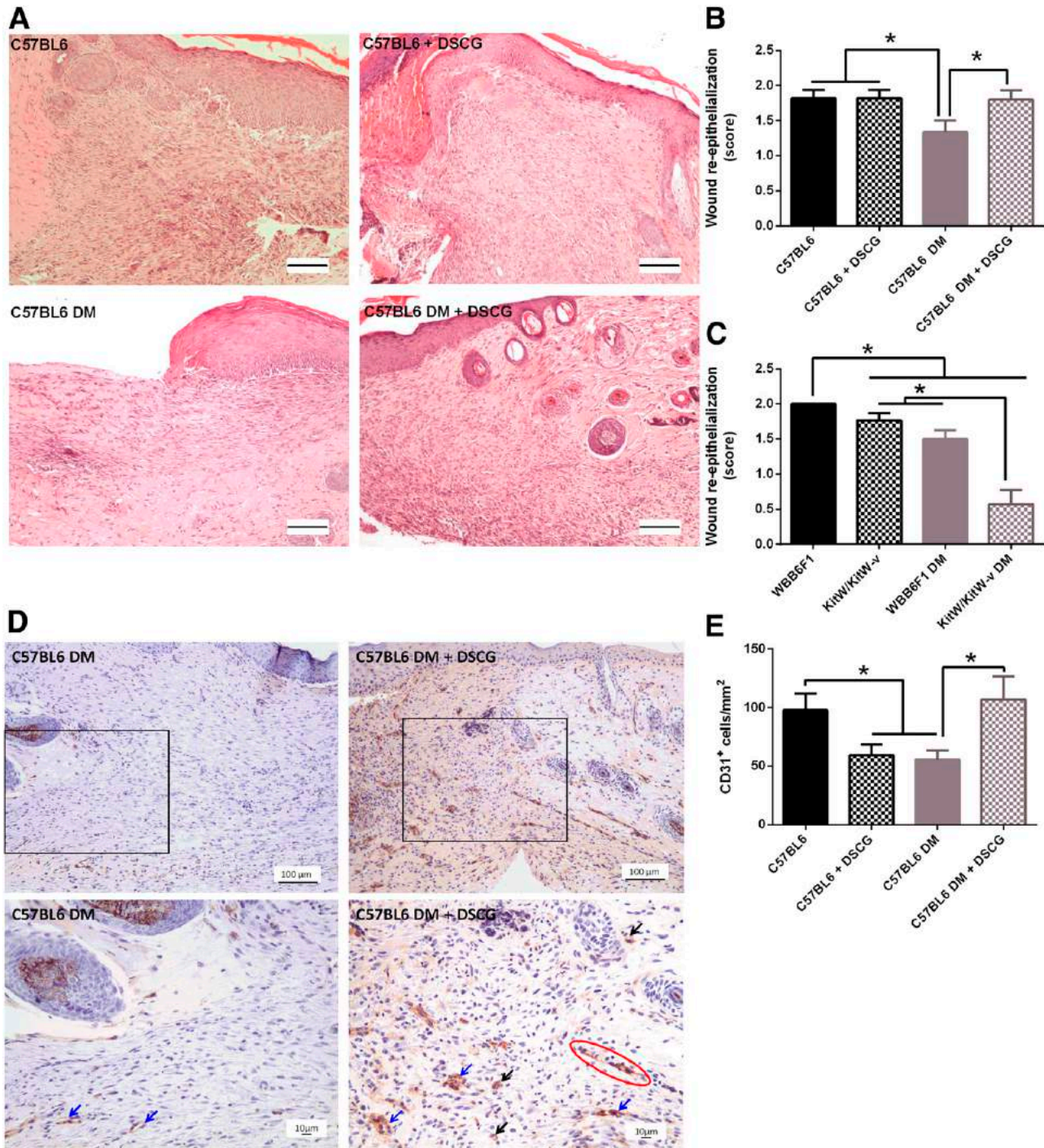


Figure 5—Wound re-epithelialization and neovascularization are reduced in diabetic (DM) mice and in *Kit^W/Kit^{W-v}* mice, and DSCG improves them in diabetic mice. Wound re-epithelialization and neovascularization were evaluated by histomorphometric analysis and CD31 staining, respectively. **A:** Representative hematoxylin-eosin images of C57BL6 mice, C57BL6 mice pretreated with DSCG, C57BL6 diabetic mice, and C57BL6 diabetic mice pretreated with DSCG. Scale bar: 100 μ m. **B:** Wound re-epithelialization was reduced in C57BL6 diabetic mice when compared with both nondiabetic and diabetic DSCG-treated mice. **C:** Wound re-epithelialization was reduced in WBB6F1 diabetic mice when compared with their nondiabetic controls. Nondiabetic and diabetic *Kit^W/Kit^{W-v}* mice had lower re-epithelialization than their respective nondiabetic and diabetic WBB6F1 controls. Diabetic *Kit^W/Kit^{W-v}* mouse wounds had more incomplete re-epithelialization than nondiabetic *Kit^W/Kit^{W-v}* wounds. **D:** Representative images using CD31 staining of untreated C57BL6 diabetic mice and C57BL6 diabetic mice pretreated with DSCG, at lower (top panel) and higher (bottom panel) magnification. The red circle shows a vascular sprout, blue arrows show small-caliber blood vessels with an open lumen, and black arrows show either single CD31⁺ cells or groups of two to three CD31⁺ cells. **E:** Single CD31⁺ cells were reduced in nondiabetic DSCG-treated mice and C57BL6 diabetic mice compared with C57BL6 nondiabetic mice. Diabetic DSCG-treated mice had similar numbers of CD31⁺ cells compared with nondiabetic controls. **P* < 0.05.

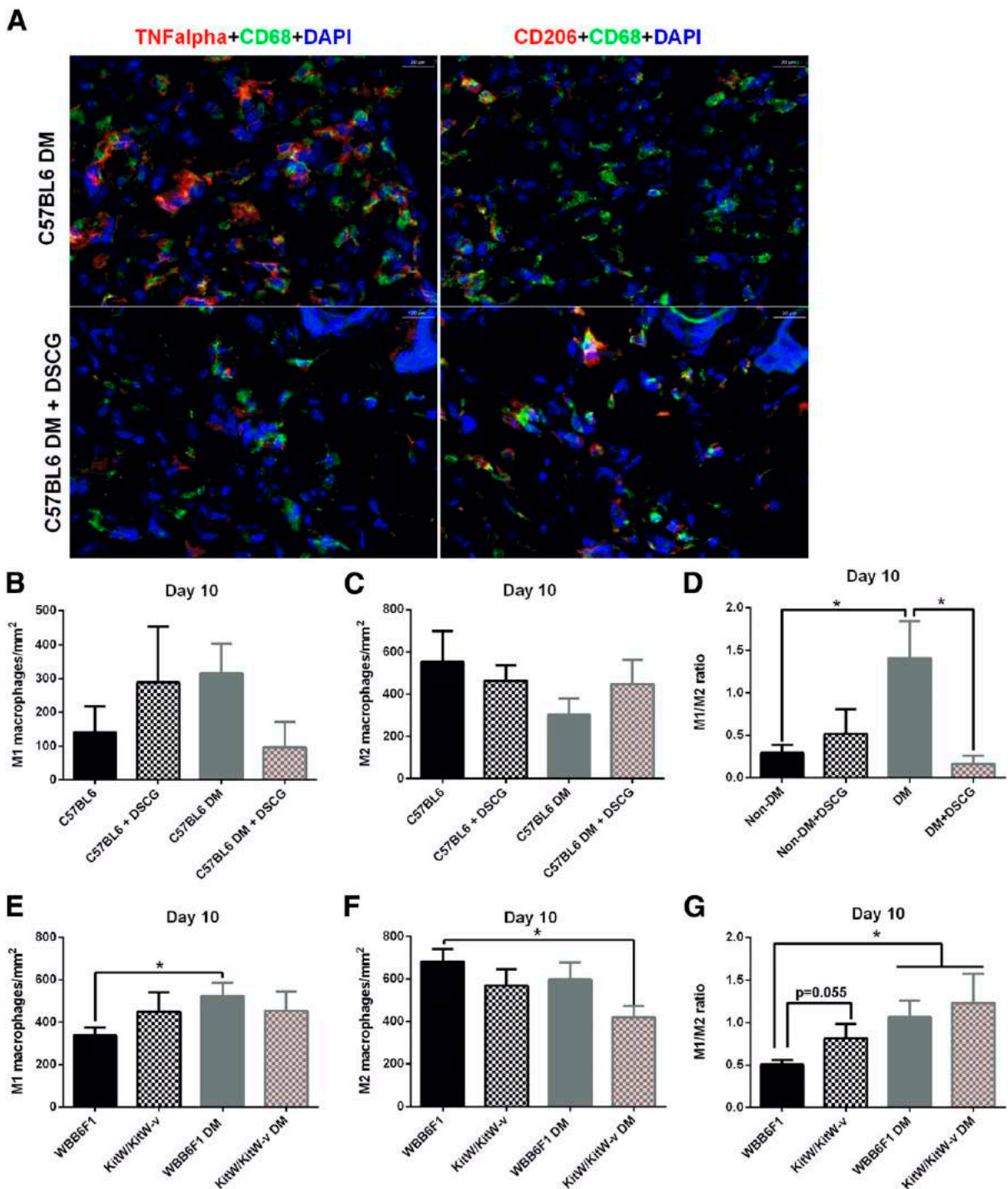


Figure 6—M1/M2 macrophage ratio is increased in the periwound skin of diabetic mice, and DSCG pretreatment restores it to normal levels. **A:** Representative image of M1 and M2 macrophages from day 10 periwound skin of C57BL/6 diabetic mice, nontreated mice, and DSCG pretreated mice. Scale bar: 20 μ m. M1 (left panel, CD68⁺TNF- α ⁺DAPI) and M2 (right panel, CD68⁺CD206⁺DAPI) are shown in yellow-orange as a result from the triple-positive staining. **B:** C57BL/6 diabetic mice tended to have elevated numbers of M1 macrophages compared with both C57BL/6 nondiabetic (Non-DM) and diabetic (DM) mice pretreated with DSCG. **C:** C57BL/6 diabetic mice tended to have reduced numbers of M2 macrophages compared with both C57BL/6 nondiabetic and diabetic mice pretreated with DSCG. **D:** C57BL/6 diabetic mice had a significantly higher periwound M1/M2 ratio than their respective nondiabetic controls. DSCG pretreatment restored the M1/M2 ratio to normal levels in diabetic mice but had no effect in nondiabetic mice. **E:** Diabetic WBB6F1 mice had elevated numbers of M1 macrophages compared with their nondiabetic controls. Nondiabetic and diabetic *Kit^W/Kit^{W-v}* mice tended to have higher counts of M1 macrophages than nondiabetic WBB6F1 mice. **F:** Diabetic *Kit^W/Kit^{W-v}* mice had reduced numbers of M2 macrophages. Nondiabetic *Kit^W/Kit^{W-v}* and diabetic WBB6F1 mice tended to have reduced numbers of M2 macrophages when compared with nondiabetic WBB6F1 mice. **G:** Diabetic WBB6F1 and diabetic *Kit^W/Kit^{W-v}* mice had higher M1/M2 ratios in the periwound skin compared with nondiabetic WBB6F1 mice. Nondiabetic *Kit^W/Kit^{W-v}* mice had a marginally increased M1/M2 ratio compared with WBB6F1 mice ($P = 0.55$). * $P < 0.05$.

(Fig. 6B) and lower numbers of M2 macrophages (Fig. 6C), resulting in a significantly elevated M1/M2 ratio, whereas DSCG restored it to levels similar to that in nondiabetic mice (Fig. 6D). We performed the same analysis in nondiabetic and diabetic *Kit^W/Kit^{W-ν}* mice, together with their respective WBB6F1/J controls (Fig. 6E–G). The M1/M2 ratio was significantly increased in the periwound skin of diabetic WBB6F1/J mice and of diabetic *Kit^W/Kit^{W-ν}* mice, whereas it was marginally ($P = 0.055$) increased in nondiabetic *Kit^W/Kit^{W-ν}* mice when compared with nondiabetic WBB6F1/J mice (Fig. 6G). We confirmed these results with additional M1 (inducible nitric oxide synthase) and M2 (arginase-1) markers (Supplementary Fig. 2).

VEGF and MMP-9 Skin Expression Is Altered in Diabetic and in MC-Deficient Mice

Because VEGF and MMP-9 participate in wound healing and can be released by different phenotypes of MCs or macrophages, we evaluated their protein and mRNA expression in the day 0 mouse skin, and in day 10 wounds from C57BL/6J nondiabetic mice and C56BL/6J diabetic mice, pretreated with DSCG or not pretreated. VEGF protein expression was reduced in wounds in C57BL/6J diabetic mice on day 10 when compared with wounds in nondiabetic mice, whereas DSCG-pretreated diabetic mice had a postwounding increase similar to that in nondiabetic mice (Fig. 7A). VEGF mRNA levels tended to increase in C57BL/6J diabetic mice pretreated with DSCG when compared with diabetic nontreated mice, although they were not statistically significant ($P = 0.07$) (Fig. 7B). MMP-9 protein expression was increased in wounds in diabetic C57BL/6J mice on day 10, but DSCG treatment reduced it (Fig. 7C). In addition, DSCG reduced MMP-9 mRNA levels in C57BL/6J diabetic mice (Fig. 7D). We also performed mRNA analysis in MC-deficient *Kit^W/Kit^{W-ν}* mice and their respective WBB6F1/J controls. VEGF mRNA expression (Supplementary Fig. 3A) was reduced in *Kit^W/Kit^{W-ν}* mice when compared with their WBB6F1/J controls, whereas MMP-9 mRNA expression was marginally increased ($P = 0.09$) (Supplementary Fig. 3B).

Cell Culture Studies

HG Does Not Trigger MC Degranulation

To study the effect of hyperglycemia on MC degranulation, we measured β -hex release in human LAD2 cells cultured in the NG or HG condition, in the absence or presence of SP. SP induced degranulation in both NG- and HG-cultured MCs, but no differences were observed between MCs cultured in NG and HG or NG plus SP and HG plus SP (Fig. 8A).

HG Reduces VEGF Release From MCs

To evaluate the effect of hyperglycemia on VEGF release from MCs, we measured VEGF release in LAD2 cells cultured in the NG or HG condition, in the absence or presence of SP. VEGF release was reduced in the HG condition compared with NG (Fig. 8B). SP did not affect VEGF release from MCs either in the NG or HG condition.

HG Increases IL-8 Release From MC in the Presence of SP

To evaluate the effect of hyperglycemia on the release of proinflammatory MC mediators, we measured the release of IL-8, TNF- α , and MCP-1 from LAD2 cells in the same conditions as above. SP increased the release of IL-8, TNF- α , and MCP-1 in both NG- and HG-cultured MCs. IL-8 release was higher in the HG plus SP condition than in the NG plus SP condition (Fig. 8C). No differences were observed in TNF- α or MCP-1 release between NG and HG conditions with or without SP (data not shown).

DISCUSSION

This is, to the best of our knowledge, the first report of increased MC degranulation in unwounded skin in humans with diabetes and diabetic mice. We have previously reported that diabetes leads to a chronic proinflammatory state both systemically and at the skin level (6,30,31) that contributes to impaired wound healing. Here we show that, in agreement with previous studies, nondiabetic mouse skin MCs undergo considerable degranulation after wounding (20,34), and we also demonstrate that this postwounding increase in MC degranulation is absent in diabetic mice, which is consistent with their inability to mount an acute inflammatory response to injury. Blocking prewounding MC degranulation with DSCG improves wound healing in diabetic mice but has no effect in nondiabetic mice, which have minimal prewounding skin MC degranulation. MCs can be activated to selectively release certain mediators that participate in wound healing, such as VEGF, without degranulation (35), and DSCG inhibits MC inflammatory mediators but not VEGF release (36).

Furthermore, we show that MC-deficient mice, with or without diabetes, have impaired wound healing when compared with their respective WT controls. Together, these results suggest that prewounding skin-intact MCs and timely postwounding degranulation are required for optimal wound healing, whereas chronic MC degranulation has effects similar to those of MC deficiency.

In the unwounded skin of patients with diabetes, macrophages are shifted toward the M1 phenotype. In diabetic mice, DSCG pretreatment restored the postwounding M1/M2 ratio to levels seen in nondiabetic mice. Although individual macrophages can simultaneously express M1 and M2 markers, we believe that our findings, which were confirmed by multiple markers, suggest that this macrophage phenotype switch may be critical for the observed improvement in wound healing. Pretreatment with DSCG also prevented the postwounding VEGF reduction and reduced the elevated MMP-9 expression in diabetic mouse wounds.

We have previously shown that SP improves wound healing in diabetes and that its skin expression is reduced in humans and mice with diabetes (31). Here we show that SP accelerates wound healing in both nondiabetic and diabetic mice only in the presence of MCs, suggesting that SP mediates its beneficial effects in wound healing, at least partially, through MCs.

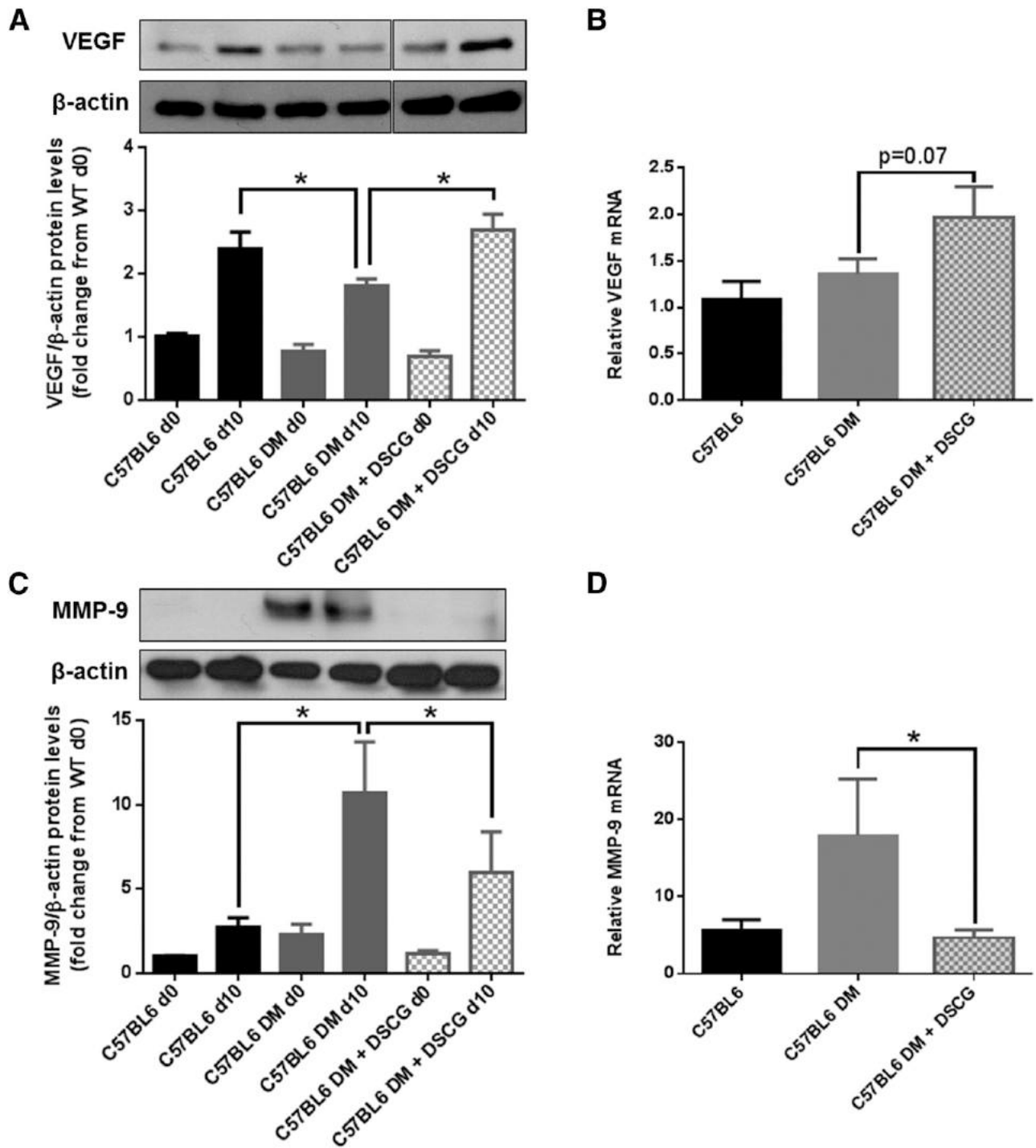


Figure 7—DSCG pretreatment increases VEGF and reduces MMP-9 skin expression in diabetic mice. Day 0 and day 10 VEGF and MMP-9 skin protein and mRNA expression from C57BL6 nondiabetic mice, nontreated C57BL6 diabetic mice (DM), and DSCG-treated C57BL6 diabetic mice were evaluated by Western blot and qRT-PCR, respectively. *A*: VEGF protein expression was reduced in wounds in diabetic C57BL6 mice on day 10, but DSCG pretreatment restored it to levels observed in nondiabetic mice. *B*: DSCG pretreatment marginally increased VEGF mRNA in C57BL6 diabetic mice ($P = 0.07$). *C*: MMP-9 protein expression was increased in both day 0 skin and day 10 wounds from C57BL6 diabetic mice when compared with their C57BL6 nondiabetic controls, and DSCG pretreatment reduced it. *D*: DSCG pretreatment reduced MMP-9 mRNA in C57BL6 diabetic mice. * $P < 0.05$ (comparisons shown in graph).

Although several studies have reported a positive role for MCs in wound healing (14,37,38), other studies (39–41) that used different MC-deficient mice or wound-healing models failed to confirm it. The reasons for this discrepancy

are not clear, but it should be emphasized that the types of MC-deficient mice used may have additional underlying defects. Moreover, the use of splinted wounds may have contributed to masking possible differences in wound closure

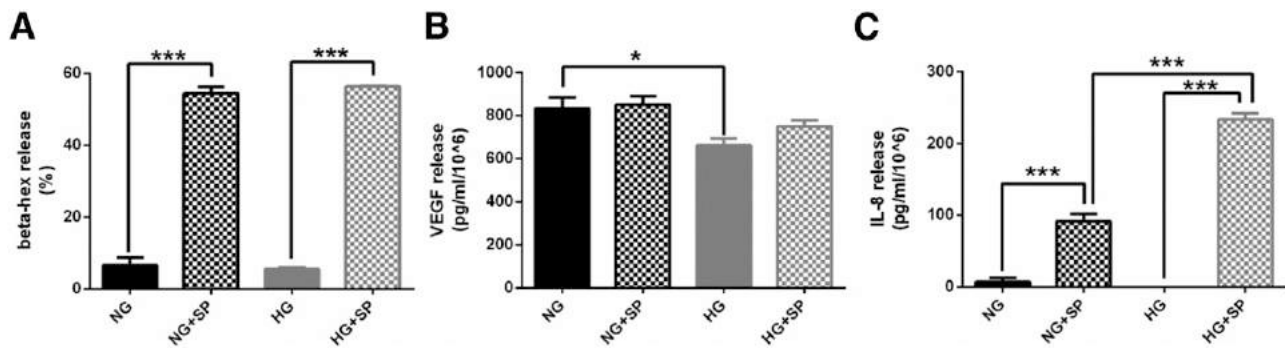


Figure 8—HG does not affect MC degranulation but influences the release of MC mediators. **A:** SP increased β -hex release from LAD2 cells cultured in NG or HG conditions. HG level did not have any effect on β -hex release. **B:** HG level reduced VEGF release from LAD2 cells. SP did not affect VEGF release from LAD2 cells, either in NG or HG conditions. **C:** SP increased IL-8 release from LAD2 cells cultured in either NG or HG conditions. No differences were observed between NG and HG conditions alone. However, IL-8 release from LAD2 cells in the HG condition and triggered with SP was 61% higher than that in the low-glucose plus SP condition. * $P < 0.05$, *** $P < 0.001$.

(42). Of note, none of these studies used diabetic mice. The only study that aimed at evaluating the role of MCs in STZ-induced diabetic mice failed to observe a solid difference in wound closure between diabetic and nondiabetic mice, but demonstrated differences in wound neovascularization and MC accumulation postinjury, suggesting that MCs participate in wound healing (43). Finally, and most importantly, none of the above-mentioned studies have used MC degranulation inhibitors in diabetic mice to provide results comparable to the ones reported here.

To further elucidate the role of MCs, we performed in vitro studies. Although hyperglycemia per se did not trigger MC degranulation, it nonetheless reduced VEGF release, one of the main factors that affect angiogenesis and wound repair. Furthermore, it increased IL-8 release, which, when chronically elevated, contributes to impaired wound healing (44–46).

The current study has its limitations. We have not identified the triggers for skin MC degranulation in humans and mice with diabetes. In addition, DSCG treatment may be affecting other cell types, as was recently reported for peripheral sensory neurons (47). However, DSCG pretreatment did not affect the release of proinflammatory mediators from human macrophages in vitro (data not shown), suggesting that it does not affect macrophage phenotype directly but rather via cross talk with MCs. Furthermore, there are well-acknowledged limitations of using kit-mutant mice to model MC deficiency. However, to date there are no reported mouse models that lack all populations of MCs while showing no MC-independent abnormalities (48). In this study, we used two of the most commonly studied mouse models of MC deficiency and the commercially available MC degranulation inhibitor DSCG. MC reconstitution of MC-deficient mice, as performed by Weller et al. (14), and additional MC degranulation inhibitors could help to better elucidate the role of MCs in wound healing in diabetes.

In summary, the main findings of the current study are as follows: 1) MC degranulation is increased in the skin of humans and mice with diabetes, 2) wound healing is

impaired in diabetic and in MC-deficient mice, and 3) pretreatment with DSCG improves wound healing in diabetic mice. Therefore, agents that prevent MC degranulation, such as luteolin and quercetin (36,49), may have the potential to improve wound healing in diabetes.

Acknowledgments. The authors thank Dr. Alexandra Miniati of the Molecular Immunopharmacology and Drug Discovery Laboratory, Department of Integrative Physiology and Pathobiology, Tufts University School of Medicine, Boston, MA, for having contributed to some of the in vitro experiments. The authors also thank Dr. Arnold S. Kirshenbaum of the National Institute of Allergy and Infectious Diseases, National Institutes of Health, Bethesda, MD, for the LAD2 cells. Finally, the authors thank Swedish Orphan Biovitrum (Stockholm, Sweden) for the generous gift of subcutaneous fat.

Funding. This work was supported by Fundação para a Ciência e a Tecnologia grants FCT-SFRH/BD/48624/2008 (to A.T.) and PTDC/SAU-FAR/121109/2010 (to A.T. and E.C.L.) and National Institutes of Health grants 1R01-DK-091949 (to J.M.Z. and A.V.), 1R01-NS-066205 (to L.P.-N. and A.V.), 1R01-DK-076937 (to A.V.), and 1R01-NS-046710 (to A.V.).

Duality of Interest. No potential conflicts of interest relevant to this article were reported.

Author Contributions. A.T. designed and performed the in vivo studies, obtained the data, and wrote the manuscript. E.C.L., M.E.A., S.K., Y.O., F.T., D.B., Y.Z., E.C., Z.W., A.Pe., A.Pa., S.P., and L.P.-N. obtained the data. A.K. performed the skin biopsy analysis. J.M.Z. supervised the breeding of the *Kit^{W-sh}/Kit^{W-sh}* mice and obtained the data. T.C.T. designed and supervised the in vitro studies, conducted the correspondent data analysis, and edited the manuscript. A.V. was responsible for the study concept and design and the initial data analysis and wrote the manuscript. All authors participated in the data analysis and interpretation processes, and reviewed and approved the final report. A.V. is the guarantor of this work and, as such, had full access to all the data in the study and takes responsibility for the integrity of the data and the accuracy of the data analysis.

Prior Presentation. Parts of this study were presented in abstract form at the 75th Scientific Sessions of the American Diabetes Association, Boston, MA, 5–9 June 2015, and at the 22nd, 23rd, 24th, and 25th Annual Meeting of the Wound Healing Society (2012, 2013, 2014, and 2016).

References

1. *Diabetes: 1996 Vital Statistics*. Vol 31. Alexandria, VA, American Diabetes Association, 1996
2. Ramsey SD, Newton K, Blough D, et al. Incidence, outcomes, and cost of foot ulcers in patients with diabetes. *Diabetes Care* 1999;22:382–387

3. Falanga V. Wound healing and its impairment in the diabetic foot. *Lancet* 2005;366:1736–1743
4. Singer AJ, Clark RA. Cutaneous wound healing. *N Engl J Med* 1999;341:738–746
5. Galkowska H, Olszewski WL, Wojewodzka U, Rosinski G, Karnafel W. Neurogenic factors in the impaired healing of diabetic foot ulcers. *J Surg Res* 2006;134:252–258
6. Dinh T, Tecilizach F, Kafanas A, et al. Mechanisms involved in the development and healing of diabetic foot ulceration. *Diabetes* 2012;61:2937–2947
7. Moon TC, St Laurent CD, Morris KE, et al. Advances in mast cell biology: new understanding of heterogeneity and function. *Mucosal Immunol* 2010;3:111–128
8. Iikura M, Suto H, Kajiwara N, et al. IL-33 can promote survival, adhesion and cytokine production in human mast cells. *Lab Invest* 2007;87:971–978
9. Sismanopoulos N, Delivanis DA, Alysandratos KD, et al. Mast cells in allergic and inflammatory diseases. *Curr Pharm Des* 2012;18:2261–2277
10. Theoharides TC, Alysandratos KD, Angelidou A, et al. Mast cells and inflammation. *Biochim Biophys Acta* 2012;1822:21–33
11. Theoharides TC, Donelan JM, Papadopoulou N, Cao J, Kempuraj D, Conti P. Mast cells as targets of corticotropin-releasing factor and related peptides. *Trends Pharmacol Sci* 2004;25:563–568
12. Egozi EI, Ferreira AM, Burns AL, Gamelli RL, DiPietro LA. Mast cells modulate the inflammatory but not the proliferative response in healing wounds. *Wound Repair Regen* 2003;11:46–54
13. Noli C, Miolo A. The mast cell in wound healing. *Vet Dermatol* 2001;12:303–313
14. Weller K, Foitzik K, Paus R, Syska W, Maurer M. Mast cells are required for normal healing of skin wounds in mice. *FASEB J* 2006;20:2366–2368
15. Younan G, Suber F, Xing W, et al. The inflammatory response after an epidermal burn depends on the activities of mouse mast cell proteases 4 and 5. *J Immunol* 2010;185:7681–7690
16. Chen R, Fairley JA, Zhao ML, et al. Macrophages, but not T and B lymphocytes, are critical for subepidermal blister formation in experimental bullous pemphigoid: macrophage-mediated neutrophil infiltration depends on mast cell activation. *J Immunol* 2002;169:3987–3992
17. Qu Z, Huang X, Ahmadi P, et al. Synthesis of basic fibroblast growth factor by murine mast cells. Regulation by transforming growth factor beta, tumor necrosis factor alpha, and stem cell factor. *Int Arch Allergy Immunol* 1998;115:47–54
18. Trautmann A, Feuerstein B, Ernst N, Bröcker EB, Klein CE. Heterotypic cell-cell adhesion of human mast cells to fibroblasts. *Arch Dermatol Res* 1997;289:194–203
19. Trautmann A, Krohne G, Bröcker EB, Klein CE. Human mast cells augment fibroblast proliferation by heterotypic cell-cell adhesion and action of IL-4. *J Immunol* 1998;160:5053–5057
20. Younan GJ, Heit YI, Dastouri P, et al. Mast cells are required in the proliferation and remodeling phases of microdeformational wound therapy. *Plast Reconstr Surg* 2011;128:649e–658e
21. Theoharides TC, Sismanopoulos N, Delivanis DA, Zhang B, Hatzigelaki EE, Kalogeromitros D. Mast cells squeeze the heart and stretch the gird: their role in atherosclerosis and obesity. *Trends Pharmacol Sci* 2011;32:534–542
22. Liu J, Divoux A, Sun J, et al. Genetic deficiency and pharmacological stabilization of mast cells reduce diet-induced obesity and diabetes in mice. *Nat Med* 2009;15:940–945
23. Lopez X, Castells M, Ricker A, Velazquez EF, Mun E, Goldfine AB. Human insulin analog-induced lipatrophy. *Diabetes Care* 2008;31:442–444
24. Paus R, Theoharides TC, Arck PC. Neuroimmunendocrine circuitry of the “brain-skin connection.” *Trends Immunol* 2006;27:32–39
25. Theoharides TC, Zhang B, Kempuraj D, et al. IL-33 augments substance P-induced VEGF secretion from human mast cells and is increased in psoriatic skin. *Proc Natl Acad Sci U S A* 2010;107:4448–4453
26. Mantovani A, Sozzani S, Locati M, Allavena P, Sica A. Macrophage polarization: tumor-associated macrophages as a paradigm for polarized M2 mononuclear phagocytes. *Trends Immunol* 2002;23:549–555
27. Mosser DM, Edwards JP. Exploring the full spectrum of macrophage activation. *Nat Rev Immunol* 2008;8:958–969
28. Sindrilaru A, Peters T, Wieschalka S, et al. An unrestrained proinflammatory M1 macrophage population induced by iron impairs wound healing in humans and mice. *J Clin Invest* 2011;121:985–997
29. Novak ML, Koh TJ. Phenotypic transitions of macrophages orchestrate tissue repair. *Am J Pathol* 2013;183:1352–1363
30. Tellechea A, Kafanas A, Leal EC, et al. Increased skin inflammation and blood vessel density in human and experimental diabetes. *Int J Low Extrem Wounds* 2013;12:4–11
31. Leal EC, Carvalho E, Tellechea A, et al. Substance P promotes wound healing in diabetes by modulating inflammation and macrophage phenotype. *Am J Pathol* 2015;185:1638–1648
32. Duttlinger R, Manova K, Chu TY, et al. W-sash affects positive and negative elements controlling c-kit expression: ectopic c-kit expression at sites of kit-ligand expression affects melanogenesis. *Development* 1993;118:705–717
33. Grimbaldeston MA, Chen CC, Piliponsky AM, Tsai M, Tam SY, Galli SJ. Mast cell-deficient W-sash c-kit mutant Kit W-sh/W-sh mice as a model for investigating mast cell biology in vivo. *Am J Pathol* 2005;167:835–848
34. Chen L, Schrementi ME, Ranzer MJ, Wilgus TA, DiPietro LA. Blockade of mast cell activation reduces cutaneous scar formation. *PLoS One* 2014;9:e85226
35. Theoharides TC, Kempuraj D, Tagen M, Conti P, Kalogeromitros D. Differential release of mast cell mediators and the pathogenesis of inflammation. *Immunol Rev* 2007;217:65–78
36. Weng Z, Zhang B, Asadi S, et al. Quercetin is more effective than cromolyn in blocking human mast cell cytokine release and inhibits contact dermatitis and photosensitivity in humans. *PLoS One* 2012;7:e33805
37. Nishikori Y, Kakizoe E, Kobayashi Y, Shimoura K, Okunishi H, Dekio S. Skin mast cell promotion of matrix remodeling in burn wound healing in mice: relevance of chymase. *Arch Dermatol Res* 1998;290:553–560
38. Shiota N, Nishikori Y, Kakizoe E, et al. Pathophysiological role of skin mast cells in wound healing after scald injury: study with mast cell-deficient W/W(V) mice. *Int Arch Allergy Immunol* 2010;151:80–88
39. Willenborg S, Eckes B, Brinckmann J, et al. Genetic ablation of mast cells redefines the role of mast cells in skin wound healing and bleomycin-induced fibrosis. *J Invest Dermatol* 2014;134:2005–2015
40. Antsiferova M, Martin C, Huber M, et al. Mast cells are dispensable for normal and activin-promoted wound healing and skin carcinogenesis. *J Immunol* 2013;191:6147–6155
41. Nauta AC, Grova M, Montoro DT, et al. Evidence that mast cells are not required for healing of splinted cutaneous excisional wounds in mice. *PLoS One* 2013;8:e59167
42. Hinz B, Mastrangelo D, Iselin CE, Chaponnier C, Gabbiani G. Mechanical tension controls granulation tissue contractile activity and myofibroblast differentiation. *Am J Pathol* 2001;159:1009–1020
43. Nishikori Y, Shiota N, Okunishi H. The role of mast cells in cutaneous wound healing in streptozotocin-induced diabetic mice. *Arch Dermatol Res* 2014;306:823–835
44. Iacono JA, Collieran KR, Remick DG, Gillespie BW, Ehrlich HP, Garner WL. Interleukin-8 levels and activity in delayed-healing human thermal wounds. *Wound Repair Regen* 2000;8:216–225
45. Pradhan Nabzdyk L, Kuchibhotla S, Guthrie P, et al. Expression of neuropeptides and cytokines in a rabbit model of diabetic neuroischemic wound healing. *J Vasc Surg* 2013;58:766–775.e712
46. Lan CC, Wu CS, Huang SM, Wu IH, Chen GS. High-glucose environment enhanced oxidative stress and increased interleukin-8 secretion from keratinocytes: new insights into impaired diabetic wound healing. *Diabetes* 2013;62:2530–2538
47. Vieira Dos Santos R, Magerl M, Martus P, et al. Topical sodium cromoglicate relieves allergen- and histamine-induced dermal pruritus. *Br J Dermatol* 2010;162:674–676
48. Galli SJ. Rethinking the potential roles of mast cells in skin wound healing and bleomycin-induced skin fibrosis. *J Invest Dermatol* 2014;134:1802–1804
49. Kritas SK, Saggini A, Varvara G, et al. Luteolin inhibits mast cell-mediated allergic inflammation. *J Biol Regul Homeost Agents* 2013;27:955–959